Journal of Fluorescence (2019) 29:111–120
https://doi.org/10.1007/s10895-018-2315-3

ORIGINAL ARTICLE

Luminescence Sensitization of Eu(III) Complexes with Aromatic Schiff Base and N,N′-Donor Heterocyclic Ligands: Synthesis, Luminescent Properties and Energy Transfer

Manju Sengar[1] · Anudeep Kumar Narula[1]

Received: 19 August 2018 / Accepted: 15 October 2018 / Published online: 27 October 2018

Abstract

Five luminescent Eu(III)-4-fluoro-N-salicylideneaniline (Fsa) complexes with different N,N′- donor heterocyclic ligands (L) were synthesized (where L = 2,2′-bipyridine (bipy), 4,4′-dimethoxy-2,2′-bipyridine (dmbp), 1,10-phenanthroline (phen), 2,9-dimethyl-1,10-phenanthroline (neo) and 2,2′-biquinoline (biq)) and characterized by structural, thermal and spectroscopic analyses. The photophysical studies of the complexes viz. UV-Vis absorption spectra, emission spectra, lifetime decay curve, radiative, non-radiative transition rates and quantum yields were investigated. The photophysical properties indicated that fluorine substituted salicylideneaniline acts as a better sensitizer for Eu^{3+} ion after involvement of ancillary ligands which leads to efficient energy transfer resulted in bright red emission due to $^5D_0 \rightarrow {}^7F_2$ transition. The highest overall quantum yield (32.78%) and sensitization efficiency (75.30%) of [$Eu(Fsa)_3$neo] showed that it is a potential candidate in optical field.

Keywords Schiff base · Quantum yield · Sensitization efficiency · Lifetime decay · Azomethine

Introduction

The synthesis and photoluminescence properties of Eu(III) complexes are of considerable interest due to various application served in the field of organic light emitting diodes [1, 2], luminescent solar concentrator [3, 4], optical imaging [5, 6], MRI contrast agents [7], photocatayst [8, 9], optical chemosensors for the detection of anions [10], cations [11], compounds [12] etc.

In spectroscopy, the importance of trivalent lanthanide ions (Ln^{3+}) is due to their electronic structure. Eu(III) is one of the most emissive ion among the trivalent lanthanide ions with $^7F_0$ as ground state and $^5D_0$ long lived excited state [13].

The lanthanide ions are weak photoluminescent species due to the following reasons. (A) The poor molar absorptivities of lanthanide ions. This results in absorption of small amount of radiations by these ions on direct excitation. (B) Transitions occurring during excitation involve same f^n configuration (f-f transition) are parity (Laporte) forbidden [14]. In order to enhance absorption of radiation by the lanthanide ions, the Ln^{3+} ions are first chelated with ligands having high molar absorption coefficients. In chelated lanthanide complexes, the intense photoluminescence may be obtained by an indirect energy transfer through chromophore (ligand) by the antenna effect [15, 16]. This is called ligand enhanced luminescence and the process occurs in three steps. (i) The ligand absorbs the excitation light, (ii) the absorbed light is transferred to the Ln^{3+} ion and (iii) the Ln^{3+} ion emits light [17].

Schiff base ligands have been widely used as versatile ligands in coordination chemistry. Recently, rare earth complexes formed by Schiff base ligand have gained considerable interest due to the formation of stable complexes. The formation of stable complexes is attributed to the presence lone pair of electrons on nitrogen atom of azomethine (-N=CH) bonding in the structure [18, 19].

In the present studies on lanthanide metal complexes, five lanthanide complexes were synthesized involving 4-fluoro-N-salicylideneaniline as primary ligand and different N,N′-donor heterocyclic ligands as ancillary ligands by single pot synthesis. The synthesized complexes were characterized on the basis of different spectroscopic studies. The photophysical properties of the Eu(III) complexes were studied with the help of UV-Vis absorption, photoluminescence emission and lifetime decay

✉ Anudeep Kumar Narula
researchchemlab58@gmail.com

[1] University School of Basic and Applied Sciences, Guru Gobind Singh Indraprastha University, Sec-16 C, Dwarka, Delhi 110078, India

curve studies. The selection of ligand N-salicylideneaniline with substituted fluoro group was done because the ligand is having selective ability to coordinate with lanthanide ions and is an effective chromophore (sensitizer) for luminescence. The introduction of fluorine substituent on ligand instead of other substituents raise the energy of triplet state of the ligand to an extent equal to the energy level of Eu(III) ion and thus promoting the energy transfer process which resulted in the observation of more sensitized luminescence [20]. The ancillary ligand (N,N′-heterocyclic ligands) acts as activator. This reinforces the photoluminescence emission and satisfy the coordination number of Eu(III) ion due to synergistic effect [21, 22]. Out of all synthesized complexes, [Eu(Fsa)$_3$neo] exhibited good photophysical properties.

Experimental Section

Reagents Used

4-fluoro-N-salicylideneaniline, 2,2′-bipyridine, 4,4′-dimethoxy-2,2′-bipyridine, 1,10-phenanthroline, 2,9-dimethyl-1,10-phenanthroline and 2,2′-biquinoline were of analytical grade and procured from Sigma-Aldrich Company(USA). Anhydrous $EuCl_3$ were also of AR grade (99.99%) obtained from Sigma-Aldrich Company (USA). Methanol (Merck, India) was distilled and then used.

Instruments Used

Carbon, hydrogen and nitrogen were analyzed by Thermofinnigan Italy 1112 series elemental analyzer. UV-Vis spectral analyses of Schiff base ligand and N,N′-heterocyclic ligands along with the complexes were carried out on Hitachi U-2900 spectrophotometer. FT-IR spectra were recorded on Shimadzu IR Affinity 1S spectrophotometer as KBr pellets. Thermal analysis were carried out using Exstar SII 6300 thermogravimetric analyzer with a heating rate of 10 °C min^{-1} from 50 °C to 800 °C taking Al_2O_3 as reference. X-ray diffraction pattern were obtained in the range of 10°-80° using Cu Kα radiation (λ = 1.54A°) with the help of Rigaku Ultima X-ray diffractometer. Scanning electron microscope (SEM) images were obtained using an EVO 18 high resolution scanning electron microscope from Carl Zeiss (Germany). The photoluminescence measurements were conducted on Varian Cary Eclipse fluorescence spectrophotometer equipped with quartz cuvettes of 1 cm path length. Time resolved PL lifetime graphs were recorded with the help of an Edinburgh instrument equipped with microsecond flash lamp using time-correlated single photon counting technique.

Synthetic Procedure

The synthesis of complexes was carried out by single pot synthesis. An anhydrous methanolic solution (10 mL) of 4-fluoro-N-salicylideneaniline (0.6456, 3 mmol) was added dropwise to a vigorously stirred solution of 2,2′-bipyridine (0.1561, 1 mmol) in 10 mL methanol. To this solution of ligands, a methanolic solution of $EuCl_3$ (0.2583 g, 1 mmol) was added slowly with continuous stirring. The pH of the reaction mixture obtained was adjusted to 6.0–7.0. After adjusting the pH, the reaction mixture was refluxed at 60 °C. The refluxing was continued for 5 h. The light yellow solution so obtained was evaporated at room temperature to give the solid compound which was extracted with diethyl ether. The compound obtained after extraction is **C1** (Scheme 1).

Similar procedure was used for the synthesis of other complexes by mixing requisite amount of Fsa, ancillary ligands and $EuCl_3$. The combination of Fsa, dmbp and $EuCl_3$ was used for the synthesis of C2. Similarly, the combination of Fsa, phen and $EuCl_3$ for C3, Fsa, neo and $EuCl_3$ for C4 and Fsa, biq and $EuCl_3$ for C5 was used to synthesize different Eu(III) complexes. The ratio of metal to Schiff base ligand to ancillary ligand was 1:3:1 in all Eu(III) complexes.

Results and Discussion

The characterization of the synthesized luminescent Eu(III) complexes were done by using the following studies.

Solubility Results

The synthesized Eu(III) complexes were soluble in common organic solvents viz. ethanol, methanol, diethyl ether, dimethyl sulfoxide and dimethylformamide and were insoluble in tetrahydrofuran and chloroform.

Elemental Analyses

The analytical contents of carbon, hydrogen and nitrogen of all the prepared complexes (**C1**-**C5**) are listed in Table 1. The outcome of elemental analyses indicated satisfactory agreement between calculated and experimental CHN values for all the complexes.

FT-IR Spectral Studies

Infrared spectra of all the ligands and complexes (Fig. 1a,b) were obtained from 4000 cm^{-1} to 400 cm^{-1} spectral range as KBr pellets The υ(C=N) stretching frequency of Fsa occurred as a sharp band at 1595 cm^{-1}. After complexation, this υ(C=N) stretching frequency

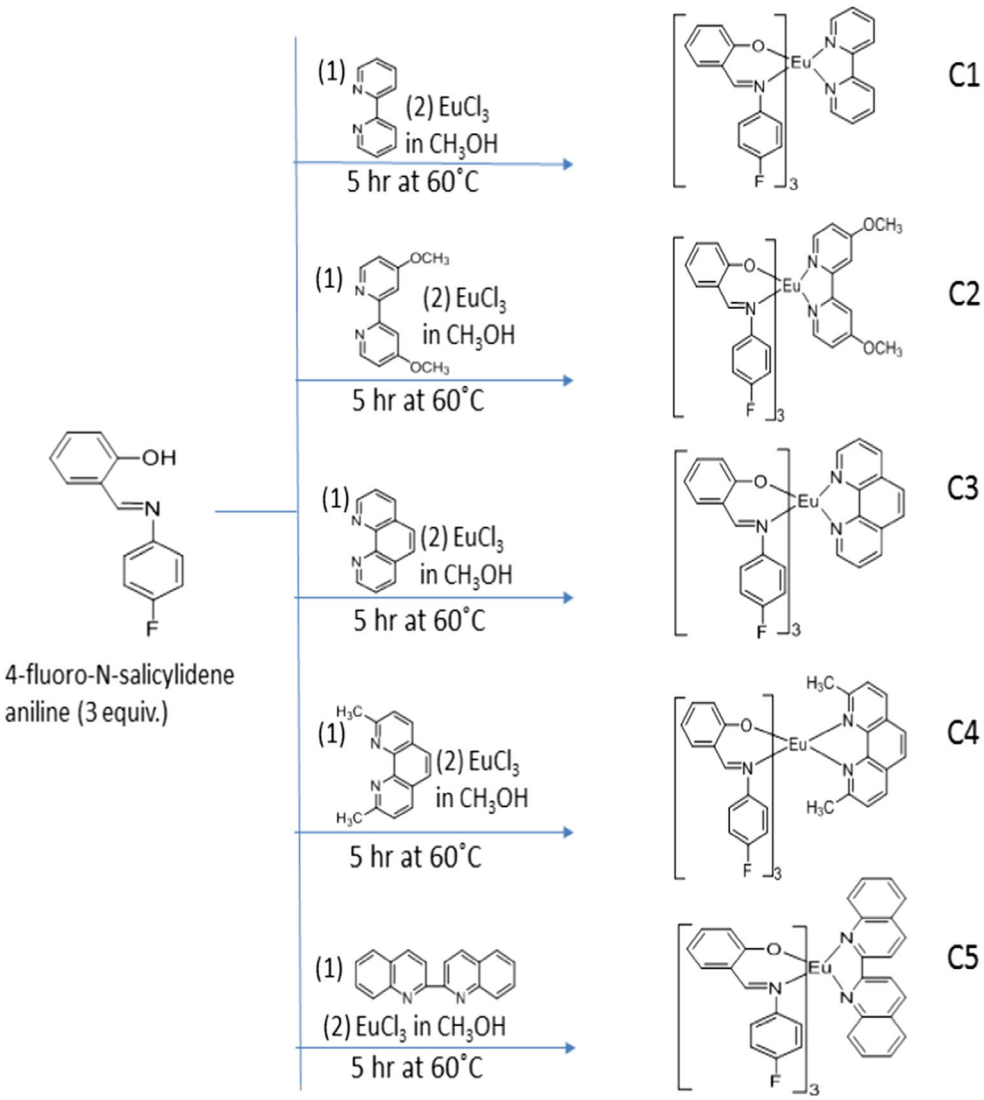

Scheme 1 Schematic representation of synthesis of europium (III) complexes

showed a shift to lower wavenumber in synthesized Eu(III) complexes suggested coordination through N-atom of azomethine group of Schiff base ligand to the Eu^{3+} ion. This shift was is confirmation with the available literature [23, 24].

Table 1 Elemental analyses results for prepared europium complexes **C1-C5**

S. No.	Formula	C% (calculated)	H% (calculated)	N% (calculated)
1.	$[Eu(Fsa)_3bipy]$	61.56 (61.89)	4.19 (4.00)	7.44 (7.36)
2.	$[Eu(Fsa)_3dmbp]$	60.25 (60.59)	3.90 (4.15)	7.03 (6.93)
3.	$[Eu(Fsa)_3phen]$	62.87 (62.83)	3.98 (3.90)	8.48 (7.18)
4.	$[Eu(Fsa)_3neo]$	63.19 (63.47)	4.00 (4.19)	6.93 (6.98)
5.	$[Eu(Fsa)_3biq]$	65.96 (65.14)	3.94 (4.00)	6.91 (6.66)

The broad absorption band due to -OH group at 3421 cm^{-1} in the FT-IR of Schiff base ligand disappeared after complex formation which indicated that O-atom of phenolic group of Schiff base ligand coordinated with Eu^{3+} ion after deprotonation.

The υ(C=N) stretching frequency of N,N′-donor heterocyclic ligands at 1579 cm^{-1} for bipy, 1585 cm^{-1} for dmbp cm^{-1}, 1587 cm^{-1} for phen, 1591 cm^{-1} for neo and 1593 cm^{-1} for biq got shifted to lower wavenumber that can be assigned to the coordination of both the N-atoms of ancillary ligands to Eu^{3+} ions. This is due to delocalization and weakening of double bonds in the conjugated chelate ring. The shift in stretching frequency υ(C=N) were in the same range in all the five complexes indicated the similar mode of coordination of Schiff base ligand in all complexes.

At lower frequency region, two distinct bands were observed in the region of 416–437 cm^{-1} and 516–522 cm^{-1} corresponding to M-N and M-O band in Eu(III) complexes respectively.

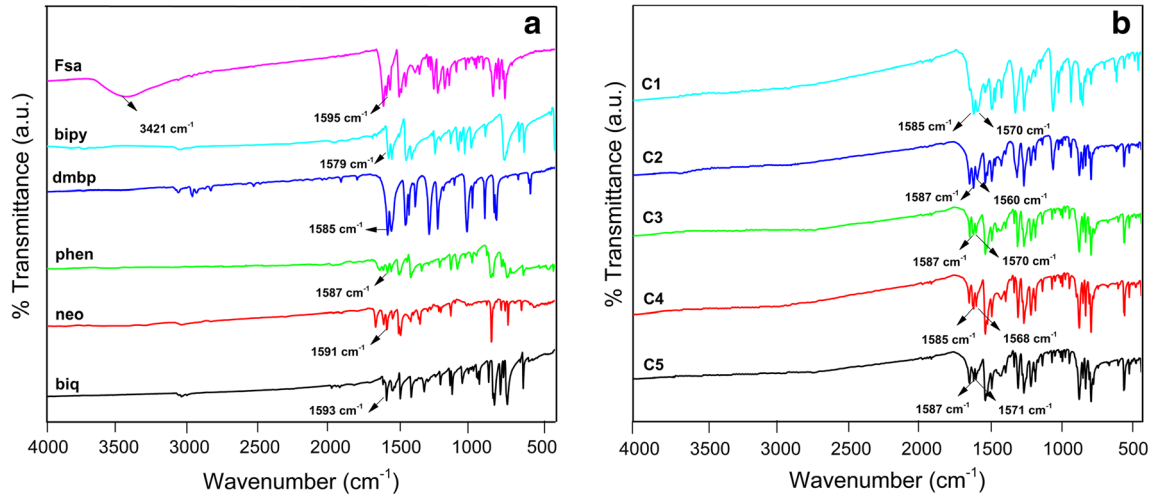

Fig. 1 **a** FT-IR spectra of primary and ancillary ligands**. b)** FT-IR spectra of synthesized Eu(III) complexes

Powdered X-Ray Diffraction Analysis

In order to understand the nature of synthesized Eu(III) complexes, powdered XRD spectra of the prepared Eu(III) complexes were recorded using CuKα radiation (λ = 1.5418 Å) at 2θ of 10°-80°. The XRD spectra of the complexes **C1**, **C2**, **C3**, **C4** and **C5** are shown in Fig. 2(a-e). The XRD spectra represented well resolved multiple peaks for all the synthesized Eu(III) complexes, indicating the crystalline nature of the complexes. The X-ray diffraction peaks (2θ) were found at 20.82°, 27.16°, 31.72°, 45.46° for **C1**, 11.52°, 14.44°, 21.78°, 28.46° for **C2**, 14.48°, 31.74°, 45.50°, 56.56° for **C3**, 13.48°, 26.24°, 31.78°, 45.40°, 51.96° for **C4** and 12.76°, 15.92°, 23.92°, 27.76°, 34.20° for **C5** complexes. In XRD spectra of complexes, variation observed in the peak position at 2θ angle for different Eu(III)-Schiff base

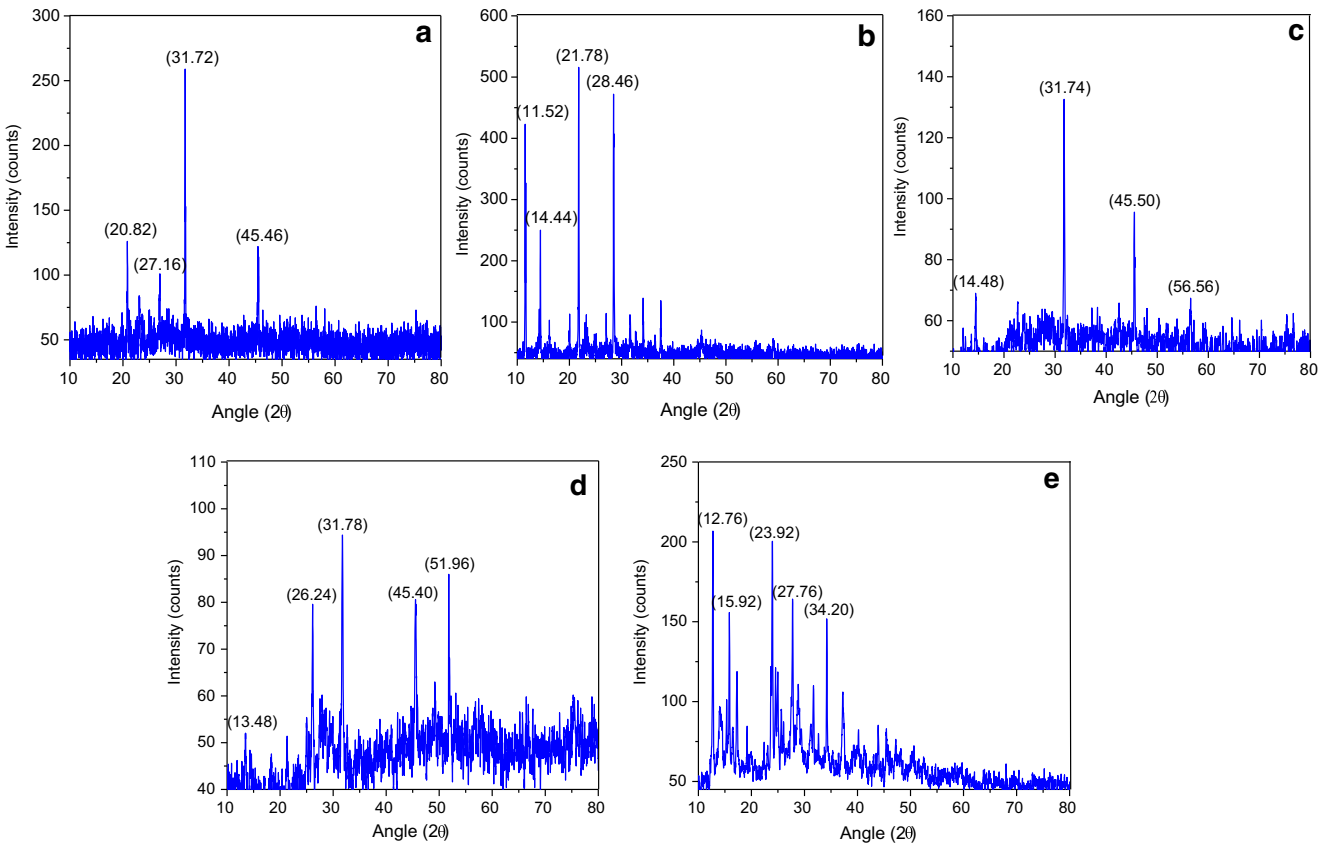

Fig. 2 XRD diffractograms of five Eu(III) complexes (**a**) [$Eu(Fsa)_3$bipy], (**b**) [$Eu(Fsa)_3$dmbp], (**c**) [$Eu(Fsa)_3$phen], (**d**) [$Eu(Fsa)_3$neo] and (**e**) [$Eu(Fsa)_3$biq] using CuKα radiation at an opening voltage of 40 kV and current of 40 mA

complexes. These results suggested that the complexes with different ancillary ligand have different structures, which can be assigned to the interaction between the Eu(III) ion and different ancillary ligands.

Scanning Electron Microscopy

The SEM micrographs (Fig. 3) were obtained to observe the morphology of prepared Eu(III) complexes. The SEM images were taken at 20.00 kV accelerating voltage and at 8.5 mm working distance. The SEM samples were prepared by spreading a finally powdered sample on carbon tape adhered to the stub and sputter coating with Au for morphology visualization. The SEM micrographs of Eu(III) complexes were obtained at a magnification of 30,000. Complex **C1** and **C2** displayed ice cube like morphology with embedded agglomerated particles in between, complex **C3** appeared as interconnected rod like morphology, complex **C4** exhibited cauliflower like morphology and complex **C5** depicted snowbush like morphology. All the complexes exhibited distinct morphology. The difference observed in the surface morphology of the prepared Eu(III) complexes due to incorporation of different ancillary ligands.

Thermogravimetric Analysis

The stability of the Eu(III) complexes towards temperature was investigated by thermogravimetric analysis at a heating of 10 °C min^{-1} in the temperature range of 50 °C–800 °C under the inert atmosphere of N_2 gas. The TG curves for the synthesized complexes are depicted in Fig. 4(a-e). The shapes of thermogravimetric curves were similar in shape and exhibited two decomposition stages.

The initial mass loss of in the TG curves of all the Eu(III) complexes can be attributed to the removal of physically adsorbed moisture.

In TG curve of **C1**, 78.89% loss in weight occurred in the first decomposition step from the starting temperature of 147 °C to ending temperature of 266 °C. Another decomposition step was observed at starting temperature of 266 °C with a weight loss of 63.43% and observed till 541 °C. These steps represented the expulsion of both the ligands. At 541 °C, the remaining mass (about 7.5%) was due to Eu_2O_3 residue.

In TG curves of other complexes, during the first decomposition step, the weight loss of 78.59%, 37.16%, 40.53% and 71.73% occurred in the temperature range of 160 °C–271 °C, 163 °C–285 °C, 151 °C–257 °C and 166 °C–293 °C for complexes **C2-C5** respectively. In the second decomposition step, the weight loss percentage were 34.65%, 63.55%, 60.38% and 20.34% in the temperature range of 271 °C–500 °C for **C2**, 285 °C–631 °C for **C3**, 257 °C–650 °C for **C4** and 293 °C–511 °C for **C5** respectively. From TG analysis it can be concluded that complexes were moderately stable towards temperature.

UV-Vis Absorption Spectral Studies

The UV-Visible spectra of ligands (Fsa, bipy, dmbp, phen, neo, biq) and corresponding europium complexes

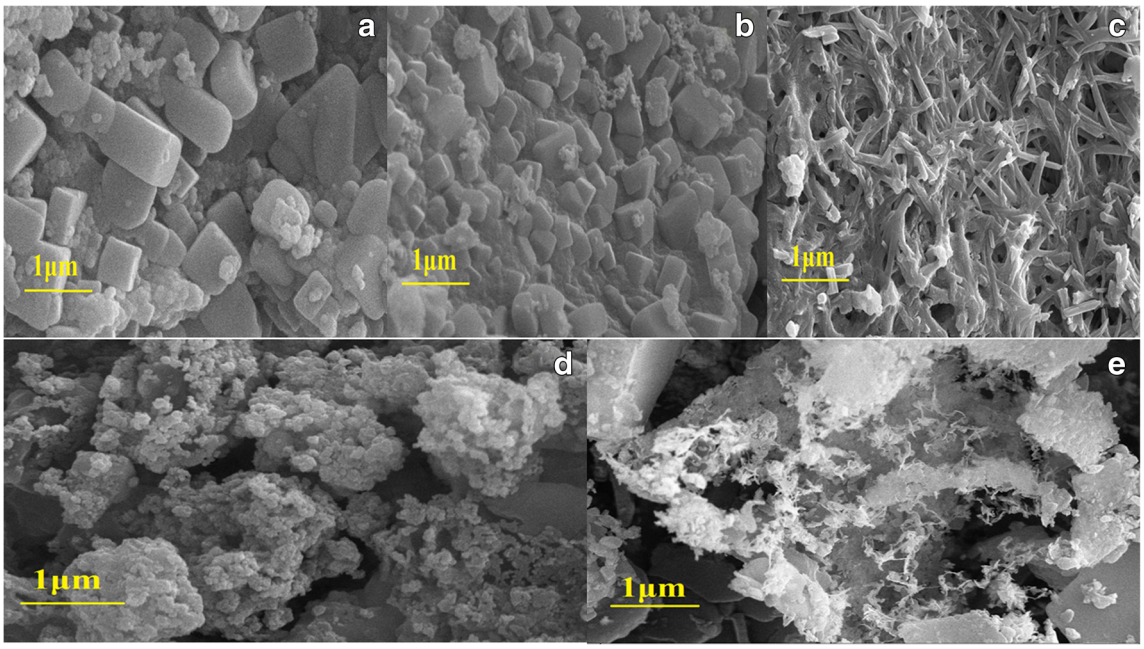

Fig. 3 Scanning electron micrographs of five Eu(III) complexes (**a**) [$Eu(Fsa)_3$bipy], (**b**) [$Eu(Fsa)_3$dmbp], (**c**) [$Eu(Fsa)_3$phen], (**d**) [$Eu(Fsa)_3$neo] and (**e**) [$Eu(Fsa)_3$biq] representing different morphologies

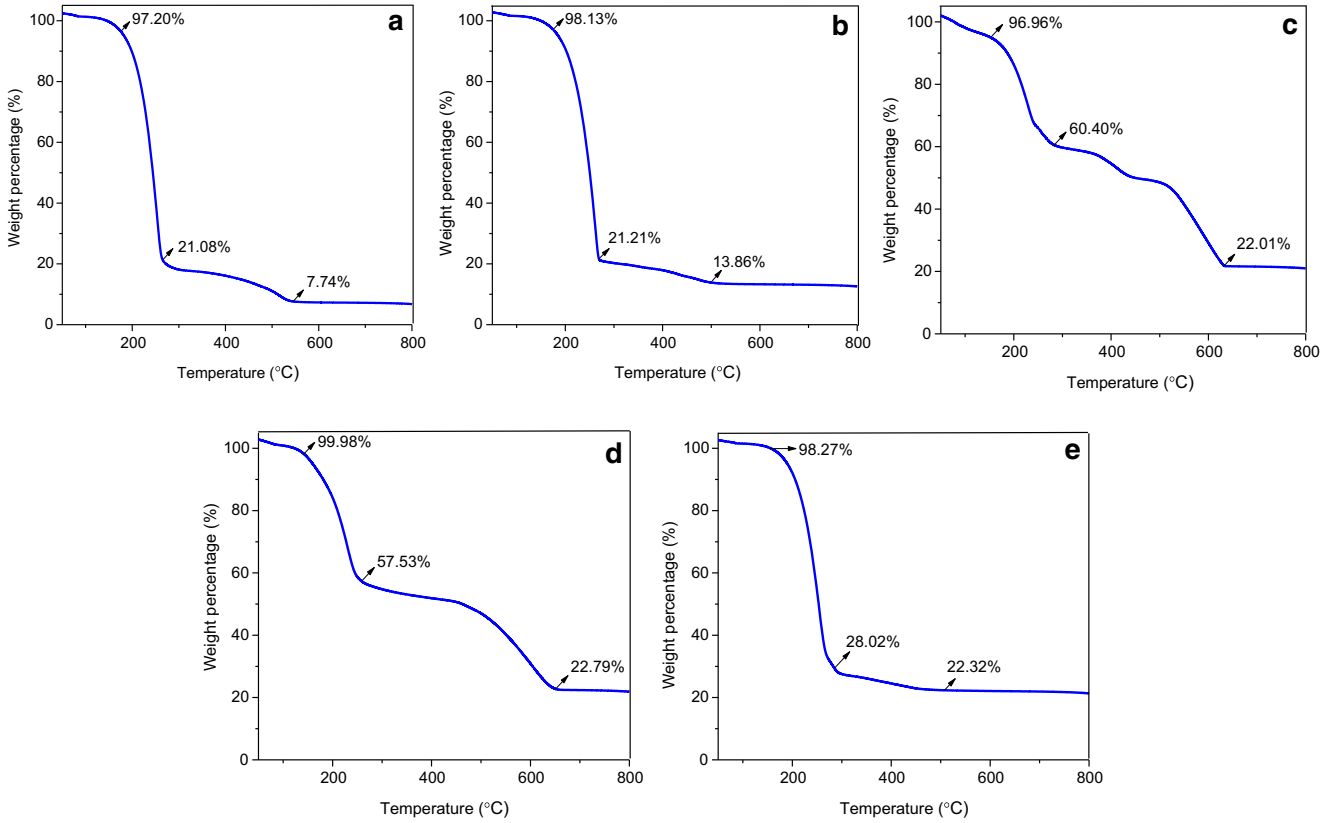

Fig. 4 Thermogravimetric curves of five Eu(III) complexes (**a**) [Eu(Fsa)$_3$bipy], (**b**) [Eu(Fsa)$_3$dmbp], (**c**) [Eu(Fsa)$_3$phen], (**d**) [Eu(Fsa)$_3$neo] and (**e**) [Eu(Fsa)$_3$biq] recorded in nitrogen atmosphere at a heating rate of 10°C min^{-1} upto 800 °C

(Fig. 5a-e) were measured in methanol (1×10^{-4} mol/L). The UV-Visible spectra showed that Fsa ligand has a good tendency to absorb light as indicated by its high absorbance value.

The Fsa ligand showed three absorption peaks at 238 nm, 252 nm and 362 nm respectively. These bands in the free Fsa were attributed to ligand transition which were $\pi \rightarrow \pi^*$ transition between double bond present in aromatic ring and $n \rightarrow \pi^*$ transition between non-bonding electrons present on nitrogen atom of azomethine group. On complexation, the absorption band due to $\pi \rightarrow \pi^*$ transition in Schiff base Eu(III) complexes shifted to longer wavelength as compared to free Fsa ligand. Another absorption band of Fsa ligand at 362 nm which was due to $n \rightarrow \pi^*$ transition undergoes a shift to lower wavelength (higher energy) as compared to one present in the free Fsa ligand.

The $\pi \rightarrow \pi^*$ transition of N,N′-donor heterocyclic ligand at 236 nm (bipy), 257 nm (dmbp), 234 nm (phen), 237 nm (neo) and 263 nm (biq) were showed a hypsochromic shift in Eu(III) complexes (233 nm (**C1**), 217 nm (**C2**), 228 nm (**C3**), 231 nm (**C4**) and 259 nm (**C5**) [25].

The clear shift in the positions of absorption bands suggested coordination of ligands to Eu(III) ion and complex formation takes place.

Photoluminescence Emission Studies and Lifetime Measurements

The photoluminescence emission spectra of the prepared Eu(III) complexes were obtained in methanol at room temperature (Fig. 6). The photoluminescence spectra of the Eu(III) complexes consist of five transitions which are $^5D_0 \rightarrow {}^7F_0$ (zero-zero band), $^5D_0 \rightarrow {}^7F_1$ (magnetic dipole), $^5D_0 \rightarrow {}^7F_2$ (induced electrical dipole), $^5D_0 \rightarrow {}^7F_3$ (magnetic dipole) and $^5D_0 \rightarrow {}^7F_4$ (induced electrical dipole) with characteristics peaks at 578, 591, 616, 653 and 699 nm for $^5D_0 \rightarrow {}^7F_J$ (J = 0–4) respectively [26]. The $^5D_0 \rightarrow {}^7F_0$ transition is non-degenerate and highly forbidden. The $^5D_0 \rightarrow {}^7F_1$ is allowed transition with weak intensity and does not depends on coordination environment around the europium ion. The hypersensitive $^5D_0 \rightarrow {}^7F_2$, transition is sensitive to the coordination environment [27]. Intense emission at 616 nm indicated that Eu(III) ion in a site without an inversion centre. The $^5D_0 \rightarrow {}^7F_3$ is forbidden and weak transition. The $^5D_0 \rightarrow {}^7F_4$ is allowed transition and its intensity is determined by the chemical composition of host matrix [28].

The time resolved photoluminescence studies of Eu(III) complexes **C1-C5** were done in methanol at room temperature and emission wavelength was kept at 616 nm. The photoluminescence lifetime graphs (Fig. 7) obtained were

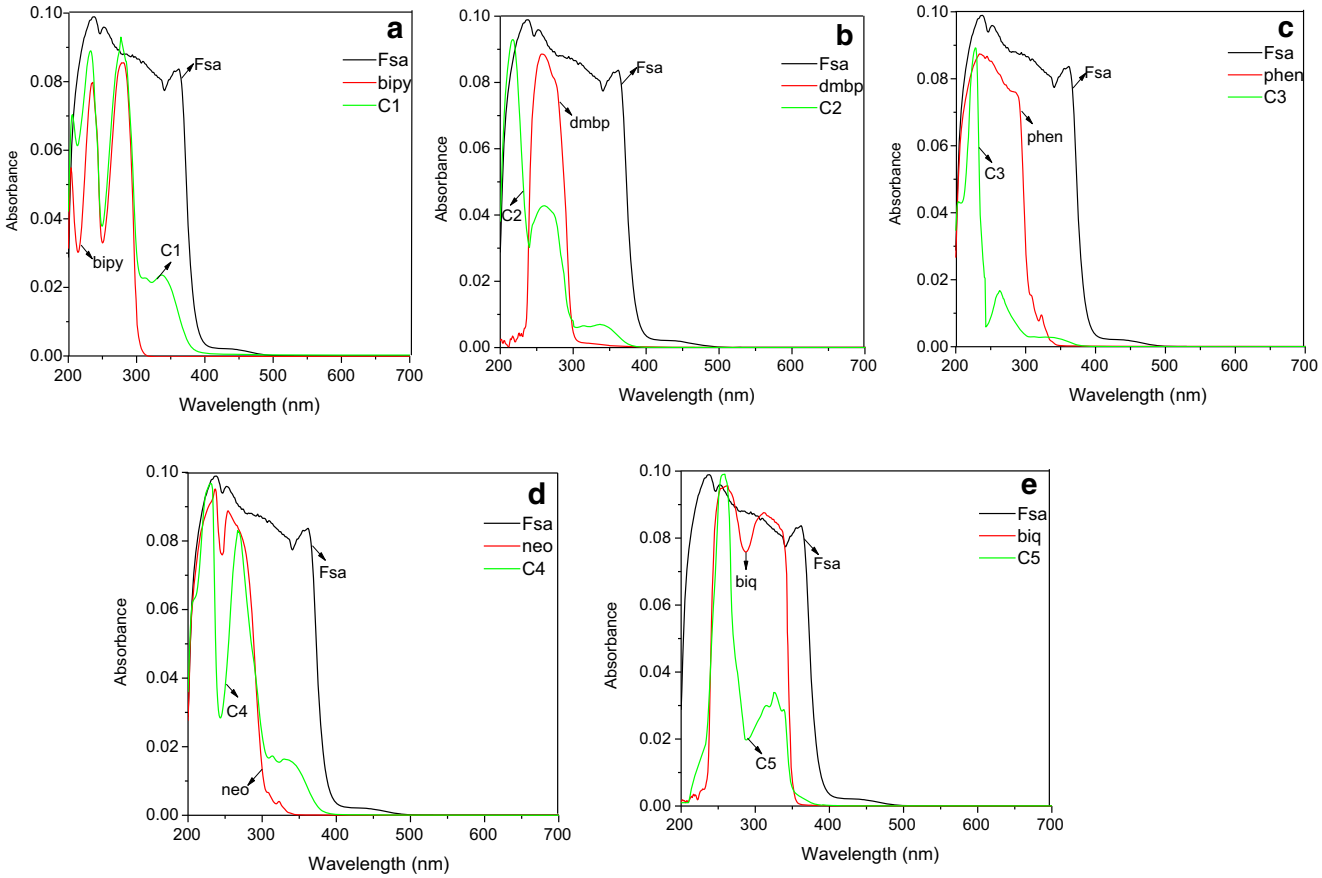

Fig. 5 **(a-e)** UV-Vis spectra of ligands and the complexes in methanol

fitted well in single exponential function suggested that all the Eu^{3+} ions were surrounded by similar average coordination environment in the prepared Eu(III) complexes [29]. The photoluminescence decay lifetime $^5D_0$ emitting levels ranges from 150 μs to 633 μs. This difference in decay lifetime is due to involvement of different ancillary ligand in complexes **C1-C5**. The photoluminescence lifetime values for the complex $[Eu(Fsa)_3neo]$ was highest among the synthesized complexes, which can be attributed to the greater sensitization efficiency value for the complex containing neocuproine as ancillary ligand.

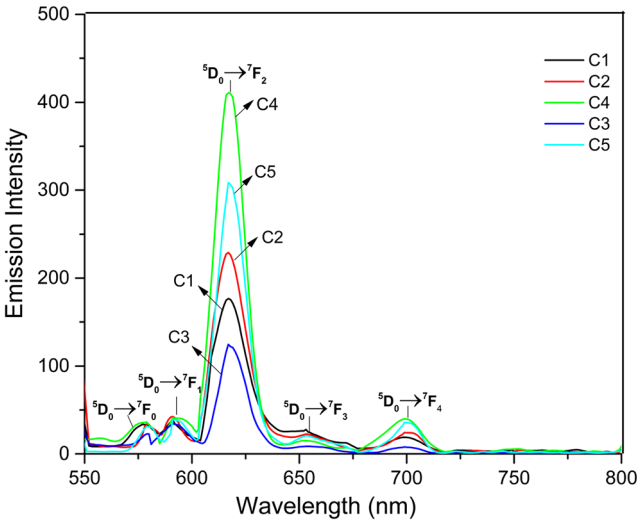

Fig. 6 Photoluminescence emission spectra of synthesized complexes in methanol at their respective excitation wavelength $\lambda_{ex} = 277$ nm for $Eu(Fsa)_3bipy$, $\lambda ex = 260$ nm for $Eu(Fsa)_3dmbp$, $\lambda ex = 263$ nm for $Eu(Fsa)_3phen$, $\lambda ex = 231$ nm for $Eu(Fsa)_3neo$ and $\lambda ex = 325$ nm for $Eu(Fsa)_3biq$

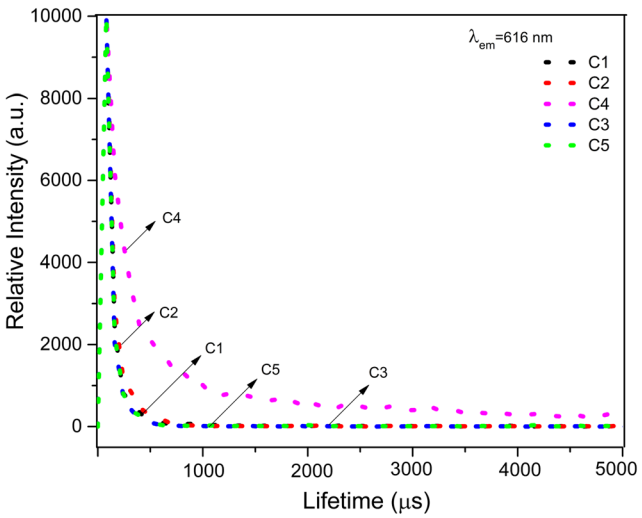

Fig. 7 Photoluminescence decay profiles observed for prepared Eu(III) complexes in methanol by monitoring emission at 616 nm

Table 2 Excitation wavelength, luminescent intensity ratio and lifetime values of europium complexes **C1-C5** at room temperature

Complex name	λex (nm)	I_2/I_1	τ(μs)
$[Eu(Fsa)_3bipy]$	277	4.53	183
$[Eu(Fsa)_3dmbp]$	260	5.38	320
$[Eu(Fsa)_3phen]$	263	3.61	150
$[Eu(Fsa)_3neo]$	231	9.98	633
$[Eu(Fsa)_3biq]$	325	7.93	380

Radiative Properties Calculation and Energy Transfer

The photoluminescence lifetimes of emission at 616 nm of the complexes were measured upon excitation in UV range at a particular wavelength. The comparison of luminescence intensities of Eu(III) complexes were made by taking the $^5D_0 \rightarrow {}^7F_2$ /$^5D_0 \rightarrow {}^7F_1$ transitions intensity ratio. Higher the value of intensity ratio, more intense is the emission of $^5D_0 \rightarrow {}^7F_2$ transition by Eu(III) ion [30]. This ratio is also used as an indicator to lanthanide site symmetry. The values for $^5D_0 \rightarrow {}^7F_2$ /$^5D_0 \rightarrow {}^7F_1$ transitions intensity ratio for complex **C1-C5** were also calculated. These results are presented in Table 2.

The photoluminescence overall quantum yield ($\Phi_{overall}$) of complexes after absorption of photon (photo-excitation of the ligand) can be calculated by the following relation [31].

$$\phi_{total} = \eta_{sens} \times \phi_{Eu} \tag{1}$$

Where η_{sens} is the efficiency of energy transfer from ligand to Ln^{3+} ion and Φ_{Eu} is the intrinsic quantum yield of the Ln^{3+} ion.

The intrinsic quantum yield of the complexes can be calculated by using the radiative and non-radiative by the expression given below

$$\phi_{Eu} = \frac{A_{rad}}{A_{rad} + Anrad} \tag{2}$$

The radiative transition rate (A_{rad}) can be calculated by the summation of Einstein's coefficient of spontaneous emission from J = 0–4 and this relation can be formulated as

$$A_{rad} = \sum A_{0J} = A_{00} + A_{01} + A_{02} + A_{03} + A_{04} \tag{3}$$

The Einstein coefficient (A_{0J}) is related to spontaneous emission of light for the transitions $^5D_0 \rightarrow {}^7F_J$ (J = 0–4) of Eu^{3+} ion and its value can be obtained by the following formula

$$A_{0J} + A_{01}\left(\frac{I_{0J}}{I_{01}}\right)\left(\frac{\nu 01}{\nu 0J}\right) \tag{4}$$

Where A_{01} is Einstein's coefficient for spontaneous emission and its value is taken as $A_{01} \approx 50\ s^{-1}$ in vacuum. A_{0J} are Einstein's coefficients between $^5D_0$ and ^7F_J (J = 0–4) energy levels. I_{01} is the integrated intensity of emission curve for the $^5D_0 \rightarrow {}^7F_1$ energy level and I_{0J} are integrated intensities of emission curve for the $^5D_0 \rightarrow {}^7F_J$ (J = 0–4) energy levels respectively and $_{01}$ and $_{0J}$ represents the energy baricenters of the $^5D_0 \rightarrow {}^7F_1$ and $^5D_0 \rightarrow {}^7F_J$ (J = 0–4) energy levels respectively.

The non-radiative transition rates (A_{nrad}), can be estimated by the following equation by using the lifetime values (τ) and radiative transition rates (A_{rad}) [32].

$$A_{tot} = \frac{1}{\tau} = A_{rad} + A_{nrad} \tag{5}$$

The overall quantum yield of luminescence (Φ_{total}) of the europium complexes **C1-C5** were measured in 10^{-6} M methanol by means of quinine sulphate in 1 N H_2SO_4 (Φ_{ref} = 0.546) as a reference at room temperature. The UV-Vis and photoluminescence emission spectra of reference quinine sulphate are represented in Fig. 8a and b respectively.

The overall quantum yields were calculated according to the equation [33].

$$\phi = \phi_{ref}\left(\frac{I}{I_{ref}}\right)\left(\frac{A_{ref}}{A}\right)\left(\frac{n^2}{n_{ref}^2}\right) \tag{6}$$

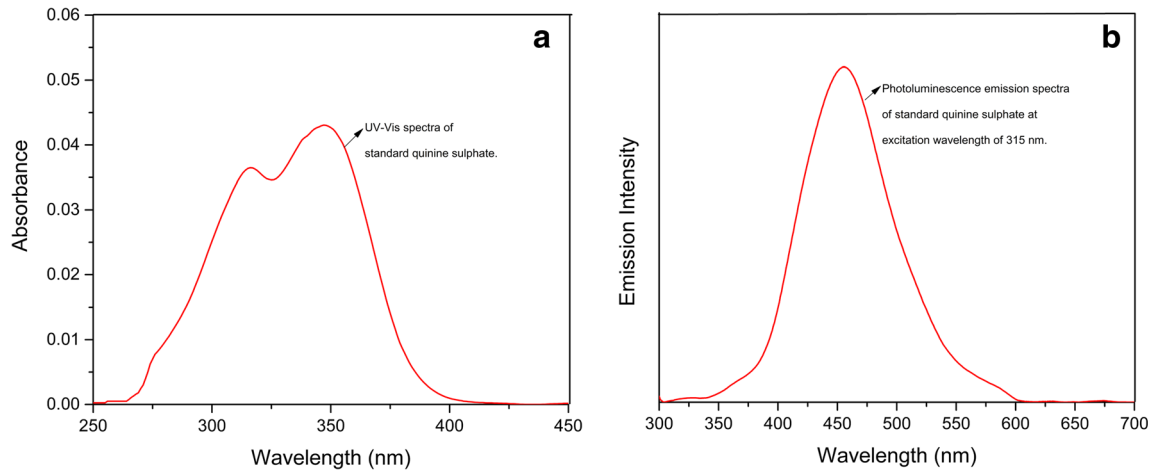

Fig. 8 **a** UV-Vis absorption spectra of quinine sulphate**. b** photoluminescence emission spectra of quinine sulphate

Table 3 Value of radiative transition rates (A_{rad}), intrinsic quantum yield (Φ_{Eu}), overall quantum yield (Φ_{total}) and sensitization efficiency (η) for complexes **C1-C5** at room temperature in methanol

Complex name	$A_{rad}(s^{-1})$	Φ_{Eu} (%)	Φ_{total} (%)	η(%)
$[Eu(Fsa)_3bipy]$	394.96	7.22	3.34	46.26
$[Eu(Fsa)_3dmbp]$	431.01	13.80	8.22	59.62
$[Eu(Fsa)_3phen]$	296.78	4.45	1.79	40.29
$[Eu(Fsa)_3neo]$	687.73	43.53	32.78	75.30
$[Eu(Fsa)_3biq]$	584.22	22.20	14.96	67.38

I represent the area of the emission spectrum of the sample, n represents the refractive index of the solvent used for sample preparation, A is the absorbance of the sample at the corresponding excitation wavelength and Φ is the overall quantum yield of sample. Subscript ref. denotes the above mentioned parameters for standard.

The photoluminescence data such as radiative transition rates, non-radiative transition rates, overall quantum yield, intrinsic quantum yield, energy transfer efficiency of europium complex were calculated by the above mentioned equations and the results are summarized in Table 3.

The bright red emission of Eu(III)-Schiff base complex involving neocuproine as ancillary ligand on excitation in UV region is due to effective intramolecular energy transfer from triplet level of ligands to emitting level of Eu(III) ion by antenna effect. The incorporation of ancillary ligand also helps in indirect energy transfer along with primary ligand in a synergistic manner.

It could be inferred from the above table that process of transfer of energy from the organic moieties (Fsa and neo) is more efficient in the case of the complex **C4.** This may be attributed to

(i). Elimination of non-radiative deactivation due to -O-H vibrations
(ii). Fsa ligand contains fluorine substituents group which enhance the spin-orbit coupling via heavy atom effect and thus boosting the intersystem crossing process [34].
(iii). neo contains two methyl group (electron donating group) which possesses better sensitization efficiency as also reported in literature [35].
(iv). Increased radiative transition rate and luminescence lifetime.

Conclusions

Five luminescent Eu(III)-Schiff base complexes were synthesized using 4-fluoro-N-salicylideneaniline ligand as suitable antenna. The coordination of ancillary ligands (N,N′-donor heterocyclic ligands) further leads to enhancement in emission intensity. The interaction of ligand's donor sites with Eu(III) ion was confirmed by FT-IR spectral studies. Optical studies suggested that the complexes possess better tendency for light absorption. All the complexes represented moderate thermal stability. The emission spectra of all Eu(III) complexes represented the hypersensitive transition at 616 nm which is responsible for red emission due to Eu(III) ion. Quantum yield and luminescence decay lifetime were obtained for all complexes using emission spectroscopy. It was found that Eu(III)-Schiff base complex containing neocuproine as ancillary ligand demonstrated much higher overall quantum yield (32.78%), lifetime (633 μs) and sensitization efficiency (75.30%). The reason for better photophysical properties exhibited by $[Eu(Fsa)_3neo]$ is the presence of electron donating methyl ($-CH_3$) group on phenanthroline moiety in neocuproine that enhances the emission intensity which in turn increases the sensitization efficiency of the complex **C4**. The above studies also indicated that fluoro substituted Schiff base ligand (Fsa) act as a better sensitizer. These results concluded that both the ligands (Fsa and neo) in a synergistic manner can afford high luminescence performance in Eu(III)-Schiff base complex.

Acknowledgements The author is availing financial support in the form of Indraprastha research fellowship (IPRF) grant no. GGSIPU/DRC/PhD/ADM./IPRF/2015/1642 for which she acknowledge, Guru Gobind Singh Indraprastha University, New Delhi. Authors are thankful to AIRF, JNU, New Delhi, for providing assistance on photoluminescence lifetime study. The authors also acknowledge Jamia Milia Islamia, New Delhi for X-ray diffraction facility (XRD) and Indian Instrumentation Centre, IIT, Roorkee for thermogravimetric analysis facility (TGA).

References

1. Law GL, Wong KL, Tam HL, Cheah KW, Wong WT (2009) White OLED with a single-component europium complex. Inorg Chem 48:10492–10494
2. Boddula R, Vaidyanathan S (2017) White light emissive bipolar ligand and their Eu(III) complex for white/red light emitting diodes. J Photochem Photobiol A: Chemistry 347:26–40
3. Levchenko V (2018) Luminescence of europium complex enhanced by surface plasmons of gold nanoparticles for possible application in luminescent solar concentrators. J Lumin 198:5–9
4. Tonezzer M, Maggioni G, Campagnaro A, Carturan S, Quaranta A, della Pirriera M, Tauste DG (2015) Luminescent solar concentrators employing new $Eu(TTA)_3phen$-containing parylene films. Prog Photovoltaics 23:1037–1044
5. Xu D, Liu M, Huang Q, Chen J, Huang H, Deng F, Wen Y, Tian J, Zhang X, Wei Y (2018) One-step synthesis of europium complexes containing polyamino acids through ring-opening polymerization and their potential for biological imaging applications. Talanta 188: 1–6
6. Utochnikova VV, Koshelev DS, Medvedko AV, Kalyakina AS, Bushmarinov IS, Grishko AY, Schepers U, Brased S, Vatsadze SZ (2017) Europium 2-benzofuranoate: synthesis and use for bioimaging. Opt Mater 74:191–196

7. Kong J, Liu T, Bao Y, Jin K, Zhang X, Tang Q, Duan C (2013) Naphthyridine-based lanthanide complexes worked as magnetic resonance imaging constrast for guanosine 5′- monophosphate in vivo. Talanta 117:412–418
8. Choi JR, Tachikawa T, Fujitsuka M, Majima T (2010) Europium-based metal-organic framework as a photocatayst for the one-electron oxidation of organic compounds. Langmuir 20:10437–10443
9. Shuhua Y, Chengcheng S, Zhongliang S (2011) Preparation and characterization of visible-light-driven europium doped mesoporous titania photocatalyst. J Rare Earths 29:929–933
10. Pang S, Zheng Y, Zhou Z, Tan C, Wang Q, Li X (2013) From molecule to complex: design of smart fluorescent anion-sensors. Opt Mater 35:1157–1161
11. Hasegawa Y, Hieda R, Nakagawa T, Kawai T (2009) Metal-ion sensing europium(III) complexes with bidentate phosphine oxide ligands containing a 2,2′-bipyridine framework. Helv Chim Acta 92:2238–2248
12. Petrochenkova NV, Mirochnik AG, Emelina TB, Sergeev AA, Leonov AA, Voznesenskii SS (2018) Luminescent amine sensor based on europium(III) chelate. Spectrochim Acta Part A 200:70–75
13. Muller G (2009) Luminescent chiral lanthanide(III) complexes as potential molecular probes. Dalton Trans 28:9692–9707
14. Lima NBD, Dutra JDL, Goncalves SMC, Freire RO, Simas AM (2016) Chemical partition of the radiative decay rate of luminescence of europium complexes. Sci Rep 6:21204
15. EDe O, Neri CR, Serra OA, Prado AGS (2007) Antenna effect in highly luminescent Eu^{3+} anchored in hexagonal mesoporous silica. Chem Mater 19:5437–5442
16. Yip YW, Wen H, Wong WT, Tanner PA, Wong KL (2012) Increased antenna effect of the lanthanide complexes by control of a number of terdentate N-donor pyridine ligands. Inorg Chem 51:7013–7015
17. Bunzli JCG, Piguet C (2005) Taking advantage of luminescent lanthanide ions. Chem Soc Rev 34:1048–1077
18. Kamaci UD, Kamachi M, Peksel A (2017) Thermally stable Schiff base and its metal complexes: molecular docking and protein binding studies. J Fluoresc 27:805–817
19. Kamaci M, Kaya I (2015) The novel poly(azomethine-urethane): synthesis, morphological properties and application as a fluorescent probe for detection of Zn^{2+} ions. J Inorg Organomet Polym 25:1250–1259
20. Zhang B, Xao T, Lu C, Li Q, Zhu Y, Tang M, Du C, Song M (2013) Systematic study of the luminescent europium-based nonanuclear clusters with modified 2-hydroxybenzophenone ligands. Inorg Chem 52:13332–13340
21. Klink SI, Hebbink GA, Grave L, Oude Alink PGB, Van Veggel FCJM (2002) Synergistic complexation of Eu^{3+} by a polydentate ligand and a bidentate antenna to obtain ternary complexes with high luminescence quantum yields. J Phys Chem A 106:3681–3689
22. Li WX, Xin XD, Feng SY, Liu Y, Zhang J, Yang Ao B, Li YJ (2014) Fluorescence enhancement of europium (III) perchlorate by 1,10-phenanthroline on the 1-(naphthalen-2-yl)-2-(phenylsulthio)ethanone complex and luminescence mechanism. Luminescence 29:810–817
23. Listkowski A, Osinska W, Mohanraj J, Pietraszkiewicz M, Dutkiewicz G, Borowiak T (2012) Synthesis and photoluminescence properties of novel lanthanide complexes based on pyrazolone Schiff bases. Synth Met 162:1285–1291
24. Tamboura FB, Diouf O, Barry AH, Gaye M, Sall AS (2012) Dinuclear lanthanide(III) complexes with large-bite Schiff bases derived from 2,6-diformyl-4-chlorophenol and hydrazides: synthesis, structural characterization and spectroscopic studies. Polyhedron 43:97–103
25. Biju S, Ambili Raj DB, Reddy MLP, Kariuki BM (2006) Synthesis, crystal structure and luminescent properties of novel Eu^{3+} heterocyclic β-diketonate complexes with bidentate nitrogen donors. Inorg Chem 45:10651–10660
26. Vats BG, Kannan S, kumar M, Drew MGB (2017) Ligand field asymmetry controlled luminescent europium(III) and samarium(III) tris (β-diketonate) complexes of diphenyl-(2-pyridyl-N-oxide)-phosphine oxide. ChemistrySelect 2:3683–3689
27. Georges J (1993) Lanthanide-sensitized luminescence and applications to the determination of organic analytes. A review. Analyst 118:1481–1486
28. Binnemans K (2015) Interpretation of Europium(III) spectra. Coord Chem Rev 295:1–45
29. Wang LH, Wang W, Zhang WG, Kang E-T, Huang W (2000) Synthesis and luminescence properties of novel Eu-containing copolymers consisting of Eu(III)-acrylate-β-diketonate complex monomers and methyl methacrylate. Chem Mater 12:2212–2218
30. Gschneider KA Jr, Bunzli JCG, Pecharsky VK (2005) Handbook of the physics and chemistry of rare earths. North Holland, Elsevier Ltd
31. Werts MHV, Jukes RTF, Verhoeven JW (2002) The emission spectrum and the radiative lifetime of Eu^{3+} in luminescent lanthanide complexes. Phys Chem Chem Phys 4:1542–1548
32. Xiao M, Selvin PR (2001) Quantum yields of luminescent lanthanide chelates and far-red dyes measured by resonance energy transfer. J Am Chem Soc 123:7067–7073
33. Rajamouli B, Sivakumar V (2017) Effect of carbazole functionalization with a spacer moiety in the phenanthroimidazole bipolar ligand in a europium(III) complex on its luminescence properties: combined experimental and theoretical study. New J Chem 41:1017–1027
34. Hebbink GA, Grave L, Woldering LA, Reinhoudt DN, van Veggel CJM F (2003) Unexpected sensitization efficiency of the near-infrared Nd^{3+}, Er^{3+}, and Yb^{3+} emission by fluorescein compared to eosin and erythrosine. J Phys Chem A 107:2483–2491
35. Meng D, Liu F, Lian X, Yang Z, Guo D (2014) Synthesis and properties of salicylaldehyde salicyhydrazone derivatives and their europium complexes. J Fluoresc 24:1661–1669